Clarification of white-fleshed guava juice by a fixed-angle conical rotor centrifuge laboratory and characterization of continuous disk stack centrifuges

Kombele Aime Ninga
National School of Agro-Industrial Sciences, University of Ngaoundere
Steve Carly Zangue Desobgo (desobgo.zangue@gmail.com)
University Institute of Technology (UIT), University of Ngaoundere
Sirshendu De
Indian Institute of Technology
Emmanuel Jong Nso
National School of Agro-Industrial Sciences, University of Ngaoundere
Joseph Kayem
National School of Agro-Industrial Sciences, University of Ngaoundere

Research Article

Keywords: guava, juice, clarification, efficiency, lab centrifuge, continuous centrifuge

Posted Date: June 22nd, 2022

DOI: https://doi.org/10.21203/rs.3.rs-1762501/v1

Abstract

The two objectives of this paper were to determine the effect of centrifugation parameters on guava juice physicochemical characteristics and to identify operational characteristics of continuous disc-stack centrifuges based on the performance of a laboratory centrifuge. Effects of *g*-force (149g – 3731g) and centrifugation time (10 – 40min) on juice physicochemical characteristics (protein, pectin, galacturonic acid, dry matter, total soluble sugars contents; pH; electrical conductivity, clarity and particle size distribution) were assessed. Laboratory centrifuge performance was evaluated for 1343g, 2388g and 3731g. At 1343g, separation limits (x_{max}), feed flow-rates of disc-stack centrifuges and cut-off sizes (x_{50}) were determined for corresponding laboratory centrifuge operation times. Significant decrease in average particle size, protein and pectin contents was observed, contrary to juice clarity. Similar clarification efficiency was obtained for *g*-forces ≥ 1343g. x_{max} were 2669nm, 2200nm and 1783nm, with corresponding x_{50} for continuous centrifuges, 1887nm, 1556nm, 1261nm, for 20min, 30min and 40min, respectively.

1 Introduction

Guava (*Psidium guajava*) is a well-known tropical and sub-tropical fruit. Originated from USA, Columbia, Peru and Mexico, it is nowadays widely spread in different countries in Asia, Africa and South America (Ninga et al. 2021). Sometimes called "*superfruit*", it is well appreciated for its high vitamin A and C content (more than 4 times that of orange) (Akesowan and Choonhahirun 2013; Surajbhan et al. 2012). Antioxidant capacity of its phenolic compound makes it suitable to trap free radicals in human body, therefore inhibiting formation and spreading of cancer cells (Flores et al. 2015). When stored at room temperature, guava fruit's shelf-life is 3–4 days, demonstrating its high perishability.

Due to its short shelf-life, guava can be processed into juice. Ninga et al., (2018) described kinetic models of hydrolysis of pectinaceous matter of guava pulp during depectinization. The effect of enzymatic treatment of guava pulp on the physicochemical parameters of the juice were described by (Akesowan and Choonhahirun 2013; Sawinder Kaur et al. 2011; Le et al. 2012; Marcelin et al. 2017; Nguyen et al. 2013; Nso et al. 1998; Surajbhan et al. 2012). FESEM images were collected and analyzed, showing particles breakdown during depectinization of the pulp (Ninga et al. 2021).

After depectinization, some chemical interactions can take place in guava juice. Polyphenols and proteins can interact with haze or tannin formation. The former, because of their positive charge, will behave as a bridge and glue, thus implying the agglomeration of the latter (negatively charged). Tannin complexes could also be the result of polymerization of phenolic compounds into denser units (McLellan and Padilla-Zakour 2005). There could also be some interactions between proteins and oligalacturonates from pectins hydrolysis (Ninga et al. 2021; Shomer et al. 1999). These interactions can lead to particles formation coupled with stone cells, affecting juice stability during storage (Wu et al. 2005).

Depectinized guava juice should be clarified to slow down haze formation during storage. This can be done through centrifugation during which particles will settle depending on their sedimentation velocity, thus forming a pellet at the sedimentation front and leaving clearer juice. Guava juice centrifugation had been the subject of many research works. Kaur et al., (2009, 2011), Surajbhan et al., (2012), Marcelin et al., (2017) determined guava yield after centrifuging depectinized guava pulp at fixed rotation speed or *g*-force and centrifugation time. They also determined some physicochemical parameters of the juice without assessing the effect of processing conditions (*g*-force and time) on them. Moreover, clarification performance of different centrifuges used in those works was not assessed. Finally, the study of the dimensional and operational characteristics of a continuous centrifuge as a function of clarification performance of the guava juice of the laboratory centrifuge has not been done. This paper has two objectives: To determine the effect of *g*-force and centrifugation time on the physicochemical characteristics of clarified guava juice; and to identify operational characteristics of a continuous centrifuge from the clarification performance of a laboratory centrifuge.

2 Material And Methods

2.1 Biological materials

Guava fruits (*Psidium guajava*) CV Lucknown 49, were purchased from local market in Kharagpur, West Bengal, India. Degree of maturity and ripeness were selection criteria.

Pectinase (Polygalacturonase) from *Aspergillus niger* (activity: 8000–12000 U/g) was purchased from HiMedia laboratories Pvt. Ltd. (Mumbai, India).

2.2 Methods

2.2.1 Preparation of White Guava Juice for Clarification

The extraction of guava juice was done following the procedure described by Ninga et al., (2021). Preliminary steps consisted of washing and rinsing of matured ripened guava fruits with tap water, followed by removal of blemishes by trimming, manual deseeding by a 16 – mesh sieve, blending using a food processor and mixing of the puree with demineralized water at a ratio of 35% w/w. The juice obtained underwent enzymatic treatment at 45 ± 2°C under continuous stirring using a Remi Motor agitator, type RQ 122 (Elektrotechnik Ltd, Kolkata, India) at 1500rpm. Operating conditions were: enzyme concentration = 0.078 weight of dried extract / weight of initial guava pulp; incubation time = 40min. Enzyme preparation was inhibited by heat treatment of depectinized guava juice for 10min at 95 ± 2°C. The juice was cooled at room temperature, then filtered using a cheese cloth (200µm mesh size). The filtrate was collected and kept in polyethylene terephthalate (PET) bottles, and stored in the freezer for further analysis.

2.2.2 Clarification of guava juice by centrifugation

Hundred grams of filtered guava juice were weighed at room temperature in 250ml centrifuge tubes. Those tubes were introduced in the rotor of a laboratory centrifuge (Remi, R – 236M, Remi Elektronik Ltd, West Bengal, India). Centrifugation was done at 35 ± 3°C. Centrifugation speeds used were 149g (1000rpm), 597g (2000rpm), 1343g (3000rpm), 2388g (4000rpm) and 3731g (5000rpm). Centrifugation times at constant speed were 10min, 20min, 30min and 40min. At the end of centrifugation, supernatant was collected in PET plastic bottles and kept in refrigerator for further analyses; whereas the pellets were discarded.

2.2.3 Determination of process parameters and physicochemical characteristics of guava juice

2.2.3.1 Determining the yield

The extraction yield of guava juice was determined using Eq. 1:

$$\eta = \frac{m_s}{m_i} \times 100$$

1

With η: the yield of guava juice (%); m_s and m_i weights of supernatant and initial guava juice (g), respectively.

4.2.2.3.2 Particle size analysis of juice samples

The determination of the particle size of the supernatant was done at 25°C using the Zetasizer based on the principle of dynamic light scattering (Malvern, Zetasizer nano, Malvern Instruments limited, UK). For this purpose, the dispersing medium used was demineralized water. For non-centrifuged guava juice, particle size distribution was obtained with the Mastersizer 2000 E (Version 5.20, Serial Number MAL1017204, Malvern Instruments Limited, United Kingdom). Average particle sizes were determined thanks to incorporated softwares. Particle size distribution curves of the centrifuged samples were fitted with Minitab 14 software using the log-normal model to determine the relationship between frequency (%) and particle size (nm) for each operating condition (*g*-force - centrifugation time) (Eq. 2). An analysis of variance was performed to determine the significance levels of the parameters.

$$y = \frac{a}{x} \times e^{\left[-0.5 \left(\frac{\ln\left(\frac{x}{x_0}\right)}{b} \right)^2 \right]}$$

2

With *x*: particle size (nm); *y*: frequency (%). *a* and *b* are the model's constants, x_0 is the geometric average particle size.

For each operating condition, the parameters *a*, *b* and x_0 were estimated using Minitab 19.0 software and coefficients of determination were determined. The surface (%*nm) of each curve was determined by calculating the integral of log-normal models between two given particle sizes using Scientific Workplace version 5.5 software.

2.2.3.3 Determination of Dry Matter Content

The determination of the dry matter content (DM) was done as follows. In a clean empty Petri dish (initial weight M_0), 5 g of guava juice was weighed and the total weight before drying (M_1) noted. The Petri dish was placed in an oven at 105°C for 24h. After drying, Petri dishes were removed and placed in a desiccator for cooling to room temperature. Final weight of the Petri dish (after drying) was determined (M_2). The dry matter content was determined using Eq. 3:

$$DM\,(\%) = \frac{M_2 - M_0}{M_1 - M_0} \times 100$$

3

2.2.3.4 Determination of other characteristics

Total soluble sugars (TSS), galacturonic acid, pectin, proteins contents; pH and electrical conductivity were determined as described by Ninga et al. (2021).

The clarity of guava juice samples was determined by measuring their transmittance at 660nm using a UV-visible spectrophotometer (M/s Perkin Elmer, Connecticut, USA) against demineralized water as blank (Jain and De, 2016).

2.2.4 Determination of the dimensional and operational characteristics of continuous centrifuges

The objective was to determine the dimensional characteristics and feed flow-rate of a continuous centrifuge based on the performance of the laboratory centrifuge. Since the technological objective desired was centered on the supernatant (guava juice), centrifugal decanting was preferred over centrifugal dewatering (Koller 2009; Towler and Sinnott 2008). The bowl of the laboratory centrifuge used is a fixed-angle conical (truncated cone) type with a fixed angle. The type of continuous centrifuge chosen in this study is the continuous disk stack-centrifuge. This choice was justified by the geometric similarity between the rotor of the laboratory centrifuge and a disc of the disk stack centrifuge (Fig. 1). This geometric similarity leads to a similarity in particle flow through the centrifuge tube and between two consecutive discs.

The determination of dimensional and operational characteristics of continuous disc stack-type centrifuges was done following the approach described by Maybury et al., (2000). They conducted a comparative study of the clarification performance of a laboratory centrifuge and a continuous disc stack centrifuge. The goal of this research was to develop a relationship between the centrifuges' clarifying performance. The study's purpose was to use the performance of a laboratory centrifuge to predict feed flow-rates of disc stack centrifuges.

2.2.4.1 Determination of operating characteristics of the laboratory centrifuge

The centrifuge used in this study was a refrigerated and programmable fixed-angle conical rotor laboratory centrifuge (Remi, R − 236M, Remi Elektrotechnik Ltd, West Bengal, India). It was equipped with a stainless-steel truncated conical bowl (rotor) model R − 236M (Fig. 2) with six tube accommodating holes. The tubes’ inclination angle to the vertical axis was 20°.

Geometric characteristics of the rotor are given in Table 1. The determination of the clarification performance of the laboratory centrifuge required the determination of its sigma factor (Σ) or theoretical equivalent area using the equation described by Rayat et al., (2016). This represents the surface area of a gravity sedimentation tank capable of ensuring similar clarification performance to the centrifuge for the same suspension feed flow-rate (Svarovsky 2000).

Table 1
Geometrical characteristics of the rotor R − 236 M

Features	Minimum radius (mm)	Minimum study radius (mm)	Maximum radius (mm)	Average radius (mm)	Inclination angle to the vertical (°)
Values	≈ 30	≈ 54	133.5	≈ 82	20

Considering the acceleration and deceleration times negligible compared to the operating time, the sigma factor of the conical rotor laboratory centrifuge was obtained from Eq. 4. This was generated by assuming the presence of a suspension consisting mainly of the cut-off size particle (x_{50}) with equal frequency in the supernatant and the pellet. For the calculation of this area, a laminar particle fall regime was assumed, thus neglecting mass transfer phenomena during centrifugation.

$$\sum_{1} = \frac{V_1 \times \omega^2}{6 \times g \times \ln\left(\frac{2R_2}{R_1 + R_2}\right)} = \frac{V_1 \times (2\pi N)^2}{3600 \times 6 \times g \times \ln\left(\frac{2R_2}{R_1 + R_2}\right)}$$

4

With Σ_1: the sigma factor of the centrifuge (m²); *g*: the acceleration of gravity (m.s^{-2}); ω: the angular velocity (rad.s^{-1}); *N*: the rotational speed (rpm); V_1: the volume of the feed (m^3); R_1 and R_2 minimum and maximum radial distances of sedimentation from the rotor axis (m).

The sigma factor was determined for the speeds 3000rpm. 4000rpm and 5000rpm.

2.2.4.2 Determination of clarification performance of the laboratory centrifuge

This determination required that of the clarification efficiency (Eq. 5) following the procedures described by Maybury et al., (2000) with some modifications. The optical density of each sample (feed and clarified samples) was determined at 660nm using a UV-visible spectrophotometer (M/s Perkin Elmer. Connecticut. USA) against demineralized water as a blank. The centrifuged sample with the minimum optical density was used as the control.

$$CE\ (\%) = \left[1 - \left(\frac{OD_{\text{sample}} - OD_{\text{control}}}{OD_{\text{ali}} - OD_{\text{control}}}\right)\right] \times 100$$

5

With: *CE*: the clarification efficiency (%); OD_{sample}, OD_{ali} and $OD_{control}$ optical densities of the sample feed and control sample, respectively.

For centrifugation speeds 3000rpm, 4000rpm and 5000rpm, the clarification efficiency was plotted against separator capacity ($V_1/t/\lambda_{lab}\Sigma_{lab}$). V_1 is the volume of the processed sample (in m^3); λ_{lab} is the correction factor to characterize the deviation of the particle flow regime from the ideal regime in the case of the laboratory centrifuge. Σ_{lab} its theoretical equivalent area (in m²) corresponding to the centrifugation speed, and *t* the centrifugation time (in s). For laboratory centrifuges, λ_{lab} is most often equated to 1 (Boychyn et al. 2004; Maybury et al. 2000). The optical density of the feed sample was equated to 2 with respect to the detection limit of the UV-visible spectrophotometer.

2.2.4.3 Determination of maximum particle size (x_{max})

The centrifugation speed used for this purpose is 3000rpm. This choice was guided by the significant variations of the parameters observed at this speed compared to the lower speeds and the negligible variations compared to the higher speeds (4000rpm and 5000rpm).

For that purpose, a preliminary determination of probability or *grade efficiency* of each particle to settle during centrifugation if the feed was exclusively made of it was done. Particle's frequency in distribution curves of both guava feed sample and clarified juice (for 20min, 30 min and 40min) were used as well as guava yield for each centrifugation condition using Eq. 6.

$$G_t(x) = 1 - (1 - E_{T_t}) \times \frac{dF_{f_t}(x)}{dF(x)}$$

6

With $G_t(x)$: the grade efficiency corresponding to the particle of size x; $dF_ft(x)$ and $dF(x)$: frequency of the particle of size x in the centrifuged and raw guava juice, respectively; E_{Tt}: the yield of guava juice centrifuged at 3000rpm for a time t in min.

For the determination of x_{max}, grade efficiency was plotted against particle size. The particle size with the greatest grade efficiency closer to 1 was considered as the limit of separation.

2.2.4.4 Determination of dimensional and operational characteristics of a continuous centrifuge for guava juice clarification

In case of linear correlation between clarification efficiency and separator capacity, equal performance of laboratory and disc-stack centrifuges could be predicted (Eq. 7), thus enabling the determination of the feed flow-rate latter using its sigma factor and the separation capacity of laboratory centrifuge (Eq. 8) as described by Maybury et al., (2000) and Rayat et al., (2016).

$$\frac{V_1}{t\sum_{lab}\lambda_{lab}} = \frac{Q}{\sum_{ds}\lambda_{ds}}$$

7

$$Q = \frac{V_1}{t\sum_{lab}\lambda_{lab}} \sum_{ds} \lambda_{ds}$$

8

With Q, Σ_{ds} and λ_{ds}, the feed flow-rate ($m^3.s^{-1}$), the sigma factor (m^2), and the correction factor for a deviation of the flow regime from the ideal regime of the continuous disk stack centrifuge. λ for disk stack centrifuges is equal to 0.4 (Boychyn et al. 2004; Maybury et al. 2000).

Intrinsic characteristics of a disc stack centrifuges found in literature (Table 2) were used to determine their sigma factor (Eq. 9) for an equivalent g-force at 3000rpm assuming that their volume flow rate is maximum (qV_{max}).

Table 2
Characteristics of commercial disc stack centrifuges identified in the literature

Models	Manufacturers	r_{min}. r_{max} (mm)	N	Z	B (m)	θ (°)	Sources
Westfalia SAOOH	Westfalia Separator AG (Oelde. Germany)	21 ; 53	62	6	0.005	45	(Boychyn et al., 2004)
GEA OTC 2-03-107	Westfalia Separator Systems GmbH	22 ; 44	36		0.0025	40	(Cambiella et al., 2006)
SC6-06-076	Westfalia Separator (Oelde. Germany)	31 ; 62	76		0.0005	40	(Chlup et al., 2008)
Westfalia CSA-1	Westfalia Separator GmbH (Oelde. Germany)	26 ; 55	45			38.5	(Espuny, 2016)
Frau CN2S	Frau (Italy)	15 ; 54.5	51			52	(Jukkola et al., 2019)
Culturefuge 100™	Alfa Laval AB (Lund. Sweden)	36 ; 84.5	82	8	0.004	40	(Shekhawat et al., 2018)

$$\sum = \frac{2}{3} \times \frac{\omega^2}{g} \times N \times \frac{\pi \times (r_2^3 - r_1^3)}{\tan\theta} \times F_L$$

9

With Σ: the sigma factor of the centrifuge (m²); θ: inclination angle of discs from the vertical (°); g: the acceleration of gravity (m.s^{-2}); ω: the angular velocity (rad.s^{-1}); N: number of discs; F_L: the correction factor of caulks on discs; r_1 and r_2 inner and outer radii of the discs (m), respectively.

In case of available discs' specifications; F_L was determined using Eq. 10; otherwise; it was equated to 1.

$$F_L = 1 - \left(\frac{3Z_L B_L}{4\pi r_2}\right) \left(\frac{1 - \left(\frac{r_1}{r_2}\right)^2}{1 - \left(\frac{r_1}{r_2}\right)^3}\right)$$

10

With: Z_L the number of caulks on each disc; B_L: the height of a caulk (m).

Feed flow-rates of each centrifuge were determined at 3000rpm for 20min, 30min and 40min, respectively. The disk stack centrifuge with the greatest feed flow-rate of guava juice for a given operating time of the laboratory centrifuge was selected.

2.2.4.5 Determination of the theoretical cut-off size (x_{50}) for the disc stack centrifuges

Particle's theoretical grade efficiency or probability was plotted against its size for 20min, 30min and 40min at 3000rpm using Eq. 11, corresponding to disk stack centrifuges (Svarovsky 2000). The cut-off size (x_{50}) is the particle size of probability 0.5. This particle size is independent of the initial suspension.

$$G(x) = \left(\frac{x}{x_{\max}} \right)^2$$

11

With: $G(x)$: the probability corresponding to particles of size x (nm); x_{max}: the separation limits (nm).

3 Results And Discussion

3.1 Effect of centrifugation parameters on the physicochemical characteristics of guava juice

3.1.1 Effect of centrifugation parameters on the extraction yield of guava juice

Centrifugation resulted in the guava juice at a yield between 89.72 ± 0.69 and 97.07 ± 0.69% w/w (Fig. 3). The yield of juice extraction is almost 90% for all combinations of parameters applied. The juice yields obtained for 149g are around 90% (91 ± 2% w/w). For *g*-forces between 597g and 3731g, extraction yields are greater than 95%.

An increase in *g*-force does not significantly affect the yield of guava juice, regardless of centrifugation times. The maximum percentage of pellets in the initial juice is approximately 2.5 ± 0.5%.

3.1.2 Effect of centrifugation parameters on the particle size distribution of clarified guava juice

The particle size distribution of the raw guava juice shows two peaks, the first around 2250nm and the second around 90000nm (Fig. 4). It appears that the particles with size between 22440nm and 251785nm are those with the highest proportion. They account for 72.77% of particles present in the feed sample. The average particle size is 72138nm. Particles greater than that represent 45.45% of all

particles. It appears that non-centrifuged guava juice contains a broad range of large particles and aggregates which could either be those which passed through the filter cloth after enzymatic treatment or those resulting from interactions between deactivated proteins and oligogalacturonates from pectins hydrolysis (McLellan and Padilla-Zakour 2005; Shomer et al. 1999).

For centrifuged guava juice samples, the distribution is of Fischer (Fig. 5). For each centrifugal force, the increase in centrifugation time is accompanied by a progressive narrowing of the curves around the mean size. The smallest particle diameter is 68nm for all each operating condition. The particle size distribution curve for the 149g samples shows a predominance of particles with diameters between 615nm and 1718nm (Fig. 5a). The decrease in the frequency of particles of a given diameter as a function of time for a given *g*-force would reflect a decrease in the number of these particles during centrifugation. The reduction in the width of the particle size spectrum with increasing centrifugation time for a given acceleration is accompanied by an increase in the proportion of finer particles.

Solid lines on each curve represent the fitting log-normal model. Model constants for different operating conditions were determined and reported (Table 3), as well as values of the coefficient of determination and analysis of variances.

Table 3
Values of constants of the log-normal models, coefficients of determination and analysis of variances for each clarified guava juice sample

Centrifugation parameters		**Model Constants and Analysis of Variance Parameters**					
g-force	Time (min)	a	b	x_0	R^2	Value of F	Probability (p)
149g	10	15631.2303	0.3732	1142.2940	0.9991	6884.3455	< 0.0001
	20	23822.1460	0.2298	966.6824	0.9984	3815.1160	< 0.0001
	30	19769.6168	0.2612	922.6080	0.9955	1324.8144	< 0.0001
	40	11801.2795	0.4658	1040.1947	0.9990	6295.6201	< 0.0001
597g	10	15787.0226	0.3482	983.7673	0.9987	4668.9589	< 0.0001
	20	10913.1193	0.4006	806.1014	0.9980	2985.3766	< 0.0001
	30	8533.0774	0.4463	731.5867	0.9976	2477.1187	< 0.0001
	40	8068.4398	0.4746	733.1956	0.9996	16730.3293	< 0.0001
1343g	10	9094.7421	0.4892	857.2055	0.9994	9681.9720	< 0.0001
	20	7461.1000	0.3900	555.1124	0.9975	2348.0955	< 0.0001
	30	7115.7952	0.3769	505.2511	0.9966	1734.6698	< 0.0001
	40	6269.7107	0.4735	580.7774	0.9992	7287.9592	< 0.0001
2388g	10	7383.4772	0.4339	608.2819	0.9987	4756.9925	< 0.0001
	20	6075.1861	0.4797	560.3254	0.9993	8461.0370	< 0.0001
	30	5485.8938	0.4968	537.9501	0.9949	1156.6211	< 0.0001
	40	4887.3994	0.5077	495.4160	0.9973	2195.9962	< 0.0001
3731g	10	6444.7337	0.4115	508.3661	0.9991	7024.2033	< 0.0001
	20	5986.8620	0.3838	429.2792	0.9992	7350.1895	< 0.0001
	30	5034.3938	0.4840	486.5226	0.9927	811.4094	< 0.0001
	40	4235.7907	0.4733	397.8415	0.9973	2182.9271	< 0.0001

These coefficients show an acceptable fitting of the log-normal model for particle size distribution curves. The surface areas of curves were obtained by calculating the integer of each model between 68 and 3091nm and plotted for each operating condition (Fig. 6).

Centrifugation has a remarkable effect for centrifugal accelerations of 597g and 1343g on the profile of the particle size distribution curves, whereas a quasi-linear trend was observed for 149g, 2388g and

3731g (Fig. 6).

For a given *g*-force, an increase in the centrifugation time led to a decrease in the width of particle size range as displayed in the surface vs particle size curve (Fig. 6), therefore leading to a decrease in the average particle size of centrifuged guava juice samples (from 332nm to 1140nm) (Fig. 7). This could be explained by the fact during centrifugation, particles are submitted to centrifugal forces leading to their settling. According to Stokes' Law, the sedimentation velocity of a particle is a function of particle size, and the difference between the density of the particle and that of the fluid. The greater and denser the particle, the greater its sedimentation velocity. Particles would settle in the same magnitude of their sedimentation velocity, denser and larger particles settling first followed by lighter and smaller ones (Svarovsky 2000). This led to a decrease in the average particle size observed in centrifuged sample, as the result of the narrowing of particle size distribution curves. The consequence is an increase in the clarity of guava juice as described further.

Increasing *g*-force while fixing the centrifugation time led to a decrease in the average particle size of centrifuged samples and their particle size ranges (Figs. 6 and 7). This is in accordance to the result described by Chawafambira et al., (2015). The sedimentation velocity being a function of the centrifugal acceleration, increasing the *g*-force led to an increase in that velocity, thereby to the settling of particles in the same order of their velocity. Moreover frictional forces acting on the particles and decreasing their sedimentation velocity would therefore be increasingly negligible compared to the centrifugal force (Robatel and Borel 1989). An increase in *g*-force would lead to a progressive decrease in the effect of Brownian diffusion forces that act on fine particles, keeping them in suspension and opposing their sedimentation in the case of gravity sedimentation (Svarovsky 2000). Resulting supernatants (juice) contained finer particles with decreasing maximum particle sizes as the *g*-force increased.

For *g*-force ranging from 1343g to 3731g, there was no significant effect of centrifugation on the average particle size for centrifugation times greater than 20min (Fig. 7). This is similar for the surface vs particle size curves. This could be explained by the fact that there could be no significant difference in the sedimentation velocity of particles for those clarification conditions.

3.1.3 Effect of centrifugation parameters on the clarity of guava juice

The clarity of the different guava juices ranged from 0 to 68.72 ± 2.18% Transmittance. That of the feed sample was not measurable by the spectrophotometer. (Fig. 8). The effect of time and centrifugal acceleration on clarity showed a trend opposite to that of average particle size. An increase in time or centrifugal acceleration is accompanied by an increase in clarity as observed by Sagu et al., (2014).

The increase in percentage transmittance during centrifugation could be due to the increase in scattered light intensity caused by the reduction in the particle size spectrum of the colloidal particles in guava juice. The clarity of guava juice would reflect the behavior of suspended particles and macromolecules of samples towards the incident light beam at 660nm. Values of electrical conductivity revealed the

presence of charges in the samples. When a light beam passes through the sample, it could be scattered by negatively charged particles of the juice due to the presence of electric field and a diffuse layer around them. Settling of particles based on their sedimentation velocity could result in an increase in the clarity. This results in the presence of smaller particles in greater proportion in the juice. The smallest hydrodynamic diameter measured in each sample is 68nm, i.e. greater than 1/10 of measurement wavelength (660 nm) (Fig. 5). The intensity of scattered light depends on the particle size. The larger the particle, the greater the intensity of the scattered light (Malvern, 2013). Settling of larger particles results in the presence of smaller one in clarified juice. That could result in an increase in the intensity of transmitted light coming out from the cuvette. The intensity of light scattered by particles depends on their size and number. The larger the particle, the greater the intensity of the scattered light (Malvern Instruments 2013).

Guava juice samples corresponding to *g*-force 149g and 597g (10min) contained large particles ($d > 660$ nm) that could cause complete scattering of light due to multiple light scattering, resulting in a 0%Transmittance (Fig. 8). For *g*-forces ranging from 1343g to 3731g, for $t > 10$ min, particles with diameter less than 660nm accounted for 75% in each sample. Less light scattering could be observed in these samples, resulting in an increase in clarity with increasing time. The same phenomena could be observed for 597g.

For 3731g, a maximum clarity of 70%Transmittance is obtained (Fig. 8). That is almost equal to that observed by (Sagu et al. 2014) (75 %Transmittance) fter centrifugation of banana juice for 45 min at 10000g. The increase in clarity between 30 and 40min of centrifugation is not significant.

3.1.4 Effect of centrifugation parameters on the pectin content of guava juice

The pectin content of the non-centrifuged sample was 426.70 ± 34.54 mg/L. Centrifugation contributes to decrease the pectin content to a value between 238.69 and 19.23 mg/L (Fig. 9). For each *g*-force, increasing the centrifugation time led to a decrease in pectin content of clarified juice. 85% of pectin content reduction was recorded for 1343g, whereas 93 and 96% were depicted for 2388g and 3731g, respectively. That significant decrease was followed by an insignificant one, with slopes from 10 min to 40min of 1.52%, 0.84% and 0.03% for 1343g, 2388g and 3731g, respectively. For 149g and 597g, the decrease in pectin content is correlated with a decrease in the values of slopes between two consecutive time intervals.

The decrease in pectin content, just like that of average particle size, could mean that among the particles which settled during centrifugation could there be those made of pectins of pectinaceous matters. Oligogalcturonates resulting from pectins hydrolysis are negatively charged; they could therefore be subject to ionic interactions with positively charged compounds such as proteins, yielding in the formation of complex particles (Jaarsveld et al. 2005; Ninga et al. 2021). During centrifugation, these particles, depending on their size, sedimentation velocity and the clarification conditions, could settle forming the pellet. Particles in the supernatant could have a non-significant difference in affinity with

ethanol solution used to precipitate pectins and pectinaceous matters during analysis. That could explain linear decreasing trends with small values of slopes observed between 10 and 40min for 1343g, 2388g and 3731g. This corroborated with the decrease in average particle size with respective slopes 10.74%, 7.65% and 5.65% for 1343g, 2388g and 3731g (Fig. 9). This could be supported by the progressive narrowing of the particle size distribution curves around 200 nm to 1000 nm for all samples obtained using these centrifugal forces (Fig. 5).

An increase in *g*-force was accompanied by a decrease in pectin content. This corroborates with results described by Sagu et al., (2014). When centrifuging depectinized banana juice, they observed a decrease in alcohol insoluble solids (AIS) (among which pectins) with an increase in acceleration.

3.1.5 Effect of centrifugation parameters on the protein content of guava juice

The protein content of non-centrifuged guava juice is 713.24 ± 23.87 mg/L. The protein content decreases over the clarification time for all centrifugal accelerations applied (Fig. 10). For samples centrifuged at 1343g, 2388g, 3731g, after 10 min of separation, more than 45% of protein content reduction could be observed. This was followed by insignificant decrease up to 40 min (slope 5.64% and 3.46%, respectively), as can be seen with error bars. In the case of centrifugal acceleration of 597g, there is a decrease in protein content with a gradual decrease in the slope between two consecutive values of centrifugation time. This decrease is not considerable between 20min and 40min. For 149g, the decrease in protein content after the first 10min (21% of the value of the non-centrifuged guava juice) is followed by a moderate decrease (16.10% of the value at 10min) between 10 and 40min.

Protein content during centrifugation showed a similar trend to that of pectin content and particle size. Proteinaceous particles would be among those that settle during centrifugation. These particles could be the results of the complexation of protein molecules with other molecules, such as oligogalacturonates, polyphenols and chelating anions present in the milieu (Siebert 1999).

The decrease in protein content with increasing *g*-forces was also recorded by Sagu et al., (2014) in case of banana juice with protein content decreasing from 1060 mg/L to 610 to 610 mg/L with acceleration increased from 2000g to 10000g.

3.1.6 Effect of centrifugation parameters on other physicochemical characteristics of guava juice

3.1.6.1 Effect of centrifugation parameters on the total soluble sugars (TSS) and galacturonic acid content

The total soluble sugar content of the initial sample is 2.3 ± 0.0°Bx. Centrifugation results in an increase in the total soluble sugar content (Fig. 11). The total soluble sugar content of centrifuged samples is greater than that of non-centrifuged one. However, the increase in time and centrifugal acceleration does

not show a significant effect between different centrifuged samples. Centrifugation is not appropriate for separating soluble compounds from juice with a low molecular weight. This could also explain the insignificant effect of centrifugation parameters on the galacturonic acid content of guava juice (Fig. 12).

3.1.6.2 Effect of centrifugation parameters on dry matter content

The dry matter content of the initial sample is 2.85 ± 0.12% w/w. It appears that centrifugation contributes to a considerable decrease in the dry matter content of guava juice compared to the non-centrifuged one (Fig. 13). The significant decrease in dry matter content could be explained by particles sedimentation during centrifugation. Varying the centrifugation parameters does not significantly affect the dry matter content of the clarified samples (Fig. 13).

3.1.6.3 Effect of centrifugation parameters on pH value

The pH of the non-centrifuged guava juice is 3.71 ± 0.00. The pH does not vary significantly with increasing centrifugation parameters (Fig. 14). Monomers and oligomers of galacturonic acid could display buffering behavior leading to an insignificant change in pH (Ninga et al. 2021).

3.1.6.4 Effect of centrifugation parameters on electrical conductivity

Centrifugation contributes to a decrease in the electrical conductivity of the clarified samples (Fig. 15).

The electrical conductivity of the non-centrifuged guava juice is 1828.33 ± 7.51 mS/cm. Greater proportion of charged particles are present in non-centrifuged sample than in centrifuged ones with not-significant difference among them. Colloidal particles of the different samples would have electrical charges whose total does not lead to a considerable variation in conductivity regardless of the values of the clarification parameters. Conductivity of the samples is also the result of the charge of dissolved ions present in samples.

3.2. Determination of the dimensional and operational characteristics of a continuous disk stack centrifuge

3.2.1 Determination of the operating characteristics of the laboratory fixed-angle conical rotor centrifuge

Thanks to the geometrical characteristics given in Table 1, sigma factors of lab centrifuge rotor were calculated for 1343g, 2388g and 3731g; these were 0.475m², 0.844m² and 1.318m², respectively. An increase in the acceleration led to an increase in sigma factor, thus a greater sedimentation surface.

3.2.2. Determination of separation performance of the laboratory centrifuge

The clarification efficiency is an important factor in comparing the separation performance of the centrifuge for the different operating conditions. The performance of the centrifuge for different operating conditions is shown in Fig. 16.

For all centrifugal accelerations, the clarification efficiency decreases with separator capacity (Fig. 16). For the 1343g acceleration, it decreases from 95–71% for separator capacities ranging from $8.77*10^{-8}$ $m.s^{-1}$ to $3.51*10^{-7}$ $m.s^{-1}$. For 2388g and 3731g, it decreases from 98.41% to 90. 35% and from 100–95.15% for capacities ranging from $4.94*10^{-8}$ $m.s^{-1}$ to $1.97*10^{-7}$ $m.s^{-1}$ and from $3.16*10^{-8}$ $m.s^{-1}$ to $1.26*10^{-7}$ $m.s^{-1}$, respectively. Separator capacity is the ratio of feed flow-rate per unit area of sedimentation. Clarification efficiency reflects the centrifuge performance under operating conditions. It describes the behavior of a gravity sedimentation tank with a specific sedimentation area, if it was fed with a given flow-rate of guava juice. The decrease in clarification efficiency as a function of separator capacity could be explained by the increase in the amount of settled solids with the decrease in feed flow-rate. The suspension feed flow-rate being small coupled with reduced effect of leaching, its residence time in the tank would be long resulting in an increase in the amount of settled solids (Koller 2009). Moreover, an increase in *g*-force led to an increase in the clarification efficiency because of an increase in the corresponding surface area for sedimentation.

The increase of the *g*-force leads to a progressive narrowing of the scatter (Fig. 16). For each acceleration, linear regression fitting was done with R^2 values being 99.70%, 99.90% and 99.80%, for 1343g, 2388g and 3731g, respectively, with corresponding slopes $-9{,}20x10^{7}$, $-5{,}39x10^{7}$ and $-5{,}27x10^{7}$. Decreasing absolute value of slopes with increasing *g*-forces could be related to the decrease in surfaces of particle size distribution curves (Fig. 6). This is contrary to the results obtained by Boychyn et al., (2004), who explained greater absolute value of slope with narrowing of particle size distribution without showing the graph.

The linear correlation between clarification efficiency and separator capacity for each acceleration concluded that the performance of the laboratory centrifuge could be used to predict that of a continuous disc stack centrifuge with a given sigma factor (Maybury et al. 2000). The equation of regression line can be used to predict the feed flow-rate of that disc-stack centrifuge corresponding clarification efficiency.

Except the clarified juice sample at 1343g for 10 min, a difference in clarification efficiency of less than 10% was obtained for all operating conditions bestowing a similar performance for 1343g, 2388g and 3731g (Fig. 16). This is in agreement with the results observed by Maybury et al., (2000). They reported a non-significant difference in clarification efficiency at 1312g and 3870g. Moreover, this non-significant difference was also observed for several physicochemical parameters obtained with these operating conditions. 1343g was used as optimal *g*-force for further works.

3.2.3 Determination of maximum particle size (x_{max})

The grade efficiency varies from 0 to 1 for all centrifugation times (Fig. 17). The particle size range varies from 68nm to 3010nm. Grade efficiency of particle less than 893nm was assumed to be 0 due to limit of detection of the Mastersizer. Beyond 893 nm, grade efficiency increased with particle size for each centrifugation time. Depending on centrifugation conditions, there was a given particle size beyond which probability is equal to 1. It corresponds to the particle having the smallest probability to be detected in the supernatant if the feed was exclusively made of it. That is separation limit (x_{max}) and is 2669nm, 2200nm and 1783nm, for 20min, 30min and 40minutes respectively. It can be noticed that as separation time increased, limit of separation decreased. Particles bigger than the separation limit could easily be removed during centrifugation, since their probability is equal to 1 (Svarovsky 2000).

For particle diameters between 68nm and 1262nm, the probability increases steeply with the particle size (Fig. 17). For that range, an insignificant increase (less than 100 nm) in the particle size led to a significant increase in the probability (probability difference greater than 0.1). It gives information on the sensitivity of centrifugation. This can be noticed in the particle size distribution curves, since two particles of size difference less than 100 nm were having frequency difference greater than 1% (Fig. 5). During centrifugation, their sedimentation velocity can be significantly different with a rapid settling of the greater one.

Above 1262nm, the probabilities increase non-significantly towards 1 (Fig. 17). Thus, two particles with a particle size difference of 500nm have equal probabilities of being removed by centrifugation. In addition, a negligible difference in probabilities is observed with increasing centrifugation times. This corroborates with the frequencies obtained for each particle diameter (Fig. 5).

3.2.4 Determination of feed flow-rates for disc stack centrifuges of known dimensions

Sigma factors used are those corresponding to 1343g. Table 4 shows feed flow-rates for disc stack centrifuges for each run time of the laboratory centrifuge.

Table 4
Estimated feed flow-rates for each commercial disk stack centrifuges

Models	Σ Factor (m^2)	Operating time of the laboratory centrifuge (min)	Feed flow-rate of disc stack centrifuges (L/h)
Westfalia SAOOH	404.351	20	102.152
		30	68.101
		40	51.076
GEA OTC 2-03-107	204.469	20	51.655
		30	34.437
		40	25.828
SC6-06-076	857.071	20	216.523
		30	144.349
		40	108.262
Westfalia CSA-1	387.536	20	97.904
		30	65.269
		40	48.952
Frau CN2S	326.023	20	82.364
		30	54.909
		40	41.182
Culturefuge 100™	1666.380	20	420.980
		30	280.653
		40	210.490

For a given continuous centrifuge, increasing the run time of the laboratory centrifuge results in a decrease in its feed flow-rate to ensure similar performance to that of the latter (Table 4). Similarly, increasing the sigma factor results in an increase in the feed flow-rate for a given run time of the laboratory centrifuge.

For a given run time of the laboratory centrifuge, the Culturefuge 100™ model has the highest feed flow-rate. With neither centrifuge prices nor technical specifications available, the main criterion for selection was feed flow-rate. However, the choice of a disk stack centrifuge model will depend on the operator depending on the volume of sample to be processed and the corresponding feed flow-rate.

3.2.5 Determination of theoretical cut-off size (x_{50})

For each centrifugation time at 1343g, the increase in probability with increasing particle size for those smaller than x_{max} is observed (Fig. 18). For those greater than x_{max}, the probability was reduced to 1.

This curve describes the probability for particles of a given particle size to be removed by centrifugation if the initial suspension consisted exclusively of them. This is the probability that could be obtained if the guava juice was clarified using a continuous disk stack centrifuge operating at 1343g.

The cut-off size (x_{50}) corresponding to probability 0.5 was predicted. It varies for each treatment time; being 1887nm, 1556nm, 1261nm, for 20min, 30min and 40min, respectively. Increasing the centrifugation time would result in a decrease in the cut-off size. The decrease in surface area of particle size distribution curves with an increase in centrifugation time is accompanied by a decrease in the probability of particles of a specific size found in the supernatant after centrifugation.

4 Conclusion

In sum, the first objective of this paper was to determine the effect of centrifugal time and *g*-force on the physicochemical characteristics of clarified white-fleshed guava juice. The second objective was to identify the operational characteristics of a continuous centrifuge based on the performance of a fixed-angle conical rotor laboratory centrifuge. The increase in time and *g*-force contributed to a considerable decrease in protein content, pectin, average particle size and the area described by the particle size distribution curve. However, it led to a considerable increase in the clarity and total soluble sugar content of the centrifuged guava juice. The performance of commercial disc stack centrifuges was determined. The model Culturefuge 100™ was the one with the highest predicted feed flow-rate.

Declarations

Acknowledgement

The authors acknowledge The World Academy of Sciences for the advancement of science in developing countries (TWAS) and the Department of Biotechnology (DBT, India), for awarding the author Kombele Aimé Ninga, the DBT-TWAS Sandwich Post-graduate Fellowship Award to work at the Department of Chemical Engineering, IIT Kharagpur, West Bengal, India.

Conflict of interest

The authors declare that they have no conflict of interest

Author's contribution

1. **Ninga, A. K.** Ph.D. Conceived and designed the experiments; Performed the experiments; Analyzed and Interpreted the data; wrote the paper. Department of Process Engineering, National School of Agro-Industrial Sciences (ENSAI), University of Ngaoundere, P.O. Box 455, Adamaoua, Cameroon. E-mail: aningakombele@yahoo.fr

2. **Desobgo Z. S. C.**, Associate Professor. Analyzed the data; Contributed reagents/materials/analysis tools; Wrote the paper. Department of Food Processing and Quality Control, University Institute of Technology (UIT), University of Ngaoundere, Cameroon, P.O. Box 456, Adamaoua, Cameroon. Email: desobgo.zangue@gmail.com

3. **De S.**, Professor. Conceived and designed the experiments; Analyzed and Interpreted the data; Contributed reagents materials, analysis tools or data. Department of Chemical Engineering. Indian Institute of Technology, Kharagpur 721 302, India. E-mail: sde@che.iitkgp.ernet.in

4. **Nso, E. J.**, Professor. Contributed reagents/materials/analysis tools; reviewed the paper. Department of Process Engineering, National School of Agro-Industrial Sciences (ENSAI) of The University of Ngaoundere, P.O. Box 455, Adamaoua, Cameroon. E-mail: nso_emmanuel@yahoo.fr

5. **Kayem, J.**, Associate Professor. Contributed reagents/materials/analysis tools; reviewed the paper. Department of Process Engineering, National School of Agro-Industrial Sciences (ENSAI) of The University of Ngaoundere, P.O. Box 455, Adamaoua, Cameroon. E-mail: gjkayem@yahoo.fr

Funding Declaration

The World Academy of Sciences for the advancement of science in developing countries (TWAS) and the Department of Biotechnology (DBT, India), has awarded the author Kombele Aimé Ninga, the DBT-TWAS Sandwich Post-graduate Fellowship Award to work at the Department of Chemical Engineering, IIT Kharagpur, West Bengal, India.

Data Availability Statement

All the data for this work are available and nothing is hided. The data obtained respect ethics and no animal and human was used to have them

References

1. Akesowan, A., & Choonhahirun, A. (2013). Effect of enzyme treatment on guava juice production using response surface methodology. Journal of Animal and Plant Sciences, *23*(1), 114–120.
2. Boychyn, M., Yim, S. S., Bulmer, M., More, J., Bracewell, D. G., & Hoare, M. (2004). Performance prediction of industrial centrifuges using scale-down models. Bioprocess and biosystems engineering, *26*(6), 385–391. https://doi.org/10.1007/S00449-003-0328-Y/FIGURES/4
3. Chawafambira, A., StanleyT, N., & Augustine, M. (2015). Production and optimisation of mango juice clarification using a manually pressurised filter at medium scale level in Rusitu valley, Zimbabwe. *International Journal of Food and Nutritional Sciences (IJFANS)*, *4*(5), 131–136. http:/www.ijfans.com/currentissue.html. Accessed 21 May 2022
4. Flores, G., Wu, S. B., Negrin, A., & Kennelly, E. J. (2015). Chemical composition and antioxidant activity of seven cultivars of guava (Psidium guajava) fruits. Food Chemistry, *170*, 327–335.

https://doi.org/10.1016/j.foodchem.2014.08.076

5. Jaarsveld, F. P. van, Blom, M., Hattingh, S., & Marais, J. (2005). Effect of Juice Turbidity and Yeast Lees Content on Brandy Base Wine and Unmatured Pot-still Brandy Quality. South African Journal of Enology and Viticulture, *26*(2), 116–130. https://doi.org/10.21548/26-2-2126
6. Kaur, S, Sarkar, B. C., Sharma, H. K., & Singh, C. (2009). Response surface optimization of conditions for the clarification of guava fruit juice using commercial enzyme. *Journal of Food Process Engineering*, *34*.
7. Kaur, Sawinder, Sarkar, B. C., Sharma, H. K., & Singh, C. (2011). Response surface optimization of conditions for the clarification of guava fruit juice using commercial enzyme. Journal of Food Process Engineering, *34*(4), 1298–1318. https://doi.org/10.1111/j.1745-4530.2009.00414.x
8. Koller, E. (2009). Sédimentation et décantation. In *Aide-mémoire Génie chimique, 3e Edition* (Dunod., pp. 71–98). Paris: L'usine Nouvelle.
9. Le, T. T., Nguyen, V. P. T., & Le, V. V. M. (2012). Application of cellulase preparation to guava mash treatment in juice processing: optimization of treatment conditions by RSM. Asian Journal of Food and Agro-Industry, *5*(4), 284–291.
10. Malvern Instruments. (2013). *Zetasizer nano series, User manual*. UK.
11. Marcelin, O., Smith, A. B., Bonnin, E., & Brillouet, J.-M. (2017). Enzymatic Breakdown of Cell Wall Polysaccharides of Guava (Psidium GuajavaL.) Puree. IOSR Journal of Environmental Science, Toxicology and Food Technology, *11*(3), 14–23.
12. Maybury, J. P., Hoare, M., & Dunnill, P. (2000). The Use of Laboratory Centrifugation Studies to Predict Performance of Industrial Machines: Studies of Shear-Insensitive and Shear-Sensitive Materials. Biotechnology and Bioengineering, *67*(3), 265–273.
13. McLellan, M. R., & Padilla-Zakour, O. I. (2005). Juice Processing. In D. M. Barrett, L. Somogyi, & H. Ramaswamy (Eds.), *Processing Fruits: Science and Technology* (2nd ed., pp. 73–96). USA: CRC Press.
14. Nguyen, V. P. T., Le, T. T., & Le, V. V. M. (2013). Application of combined ultrasound and cellulase preparation to guava (Psidium guajava) mash treatment in juice processing: Optimization of biocatalytic conditions by response surface methodology. International Food Research Journal, *20*, 377–381.
15. Ninga, K. A., Desobgo, Z. S. C., De, S., & Nso, J. E. (2021). Pectinase hydrolysis of guava pulp: effect on the physicochemical characteristics of its juice. Heliyon, *7*(10), e08141. https://doi.org/10.1016/J.HELIYON.2021.E08141
16. Ninga, K. A., Sengupta, S., Jain, A., Desobgo, Z. S. C., Nso, E. J., & De, S. (2018). Kinetics of enzymatic hydrolysis of pectinaceous matter in guava juice. Journal of food engineering, *221*, 158–166. https://doi.org/https://doi.org/10.1016/j.jfoodeng.2017.10.022
17. Nso, E. J., Ndibewu, P., & Kayem, G. J. (1998). Reduction of viscosity of guava pulps by treatment with pectinases. Cameroon Journal of Biological and Biochemical Sciences, *8*(1), 7–16.

18. Rayat, A. C., Chatel, A., Hoare, M., & Lye, G. J. (2016). Ultra scale-down approaches to enhance the creation of bioprocesses at scale: impacts of process shear stress and early recovery stages. Current Opinion in Chemical Engineering, *14*, 150–157. https://doi.org/10.1016/J.COCHE.2016.09.012
19. Robatel, M., & Borel, P. (1989). Centrifugation – Généralités, Théorie. In *Technique de l'Ingénieur, Traité Génie des Procédés* (pp. 1–20). France.
20. Sagu, S. T., Nso, E. J., Karmakar, S., & De, S. (2014). Optimisation of low temperature extraction of banana juice using commercial pectinase. Food Chemistry, *151*, 182–190.
21. Shomer, I., Yefremov, T., & Merin, U. (1999). Involvement of proteins in cloud instability of Shamouti orange [Citrus sinensis (L.) Osbeck] juice. Journal of Agricultural and Food Chemistry, *47*(7), 2623–2631. https://doi.org/10.1021/jf9807723
22. Siebert, K. J. (1999). Protein - polyphenol haze in beverages. Food technology (Chicago), *53*(1), 54–57.
23. Surajbhan, S., Alka, S., Chetan, J., & Lambert, R. (2012). Extraction and optimization of guava juice by using response surface methodology. American Journal of Food Technology, *7*(6), 326–339. https://doi.org/10.3923/AJFT.2012.326.339
24. Svarovsky, L. (2000). Separation by centrifugal sedimentation. In *Solid – Liquid Separation* (Fourth Edition., pp. 246–280). Oxford: Butterworth – Heinemann.
25. Towler, G., & Sinnott, R. (2008). Equipment Selection, Specification, and Design. In *Couldson and Richardson's Chemical Engineering, Chemical Engineering Design (Principles, Practice and Economics of Plant and Process Design)* (Vol. Volume 6, pp. 541–639). London: Butterworth-Heinemann.
26. Wu, J. S.-B., Wu, M.-W., & Wei, Y.-P. (2005). Tropical Fruits. In D. M. Barrett, S. L., & H. Ramaswamy (Eds.), *Processing Fruits: Science and Technology* (Second Edi., pp. 679–705). USA: CRC PRESS.

Figures

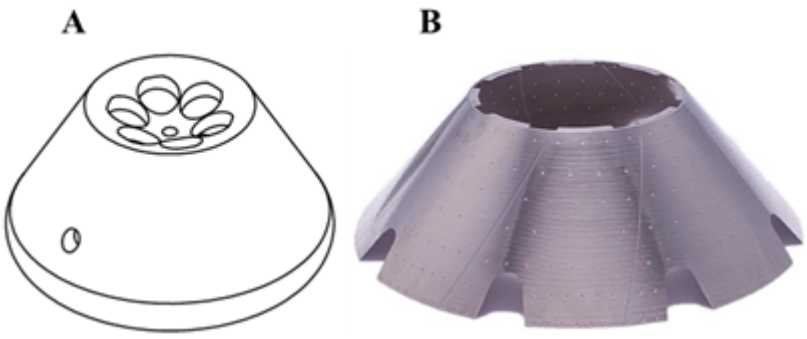

Figure 1

Three-dimensional representation of (A) the rotor of a laboratory fixed-angle conical rotor centrifuge and (B) a disc of a disc stack centrifuge (Alpha Laval)

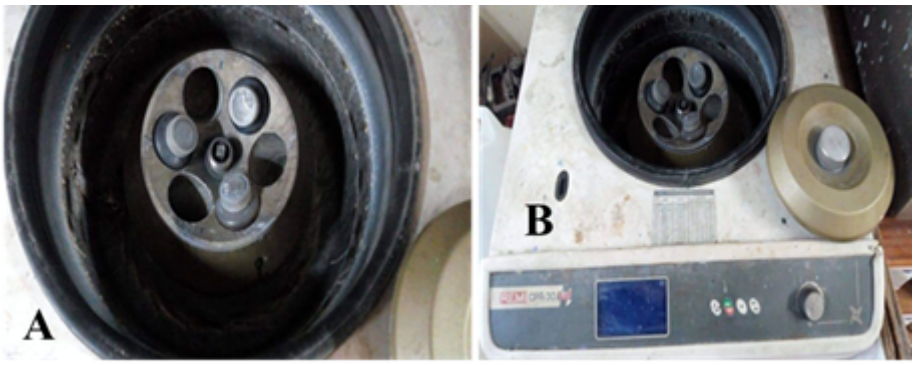

Figure 2

Image of the R - 236M rotor (A) and the laboratory fixed-angle conical rotor centrifuge (B)

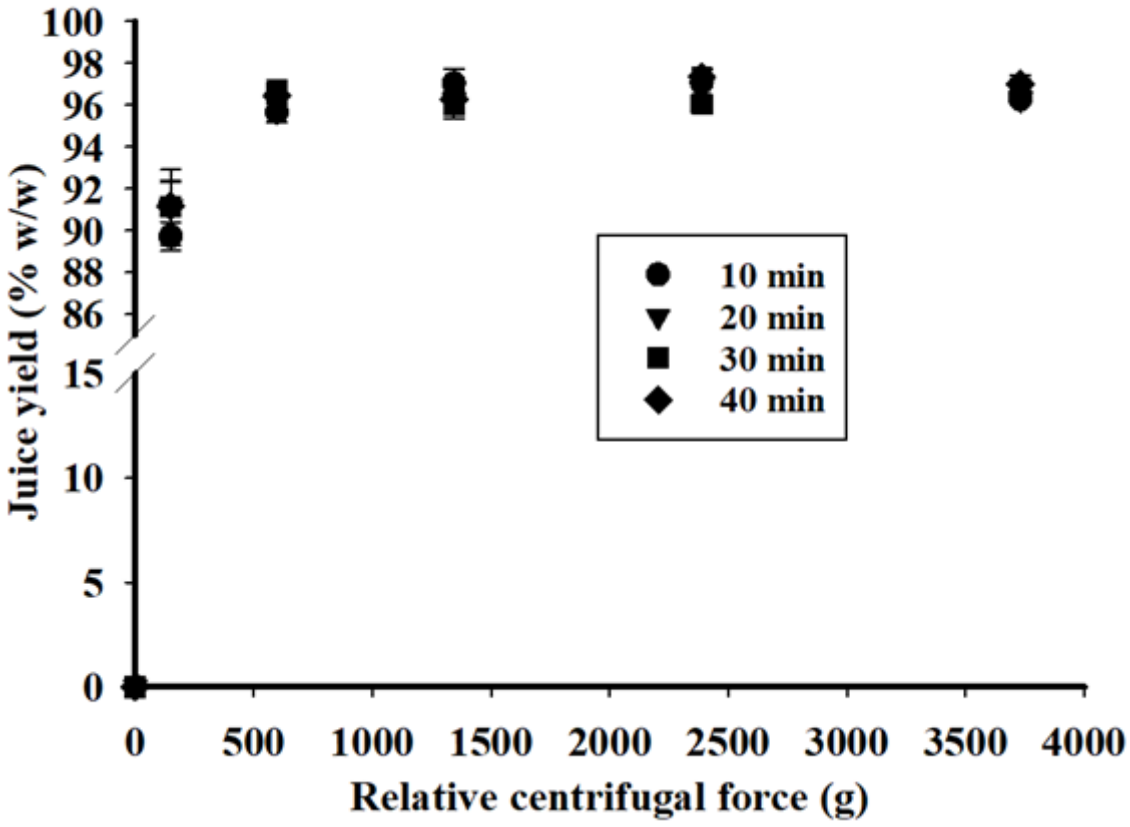

Figure 3

Yield of guava juice as a function of the relative centrifugal force applied

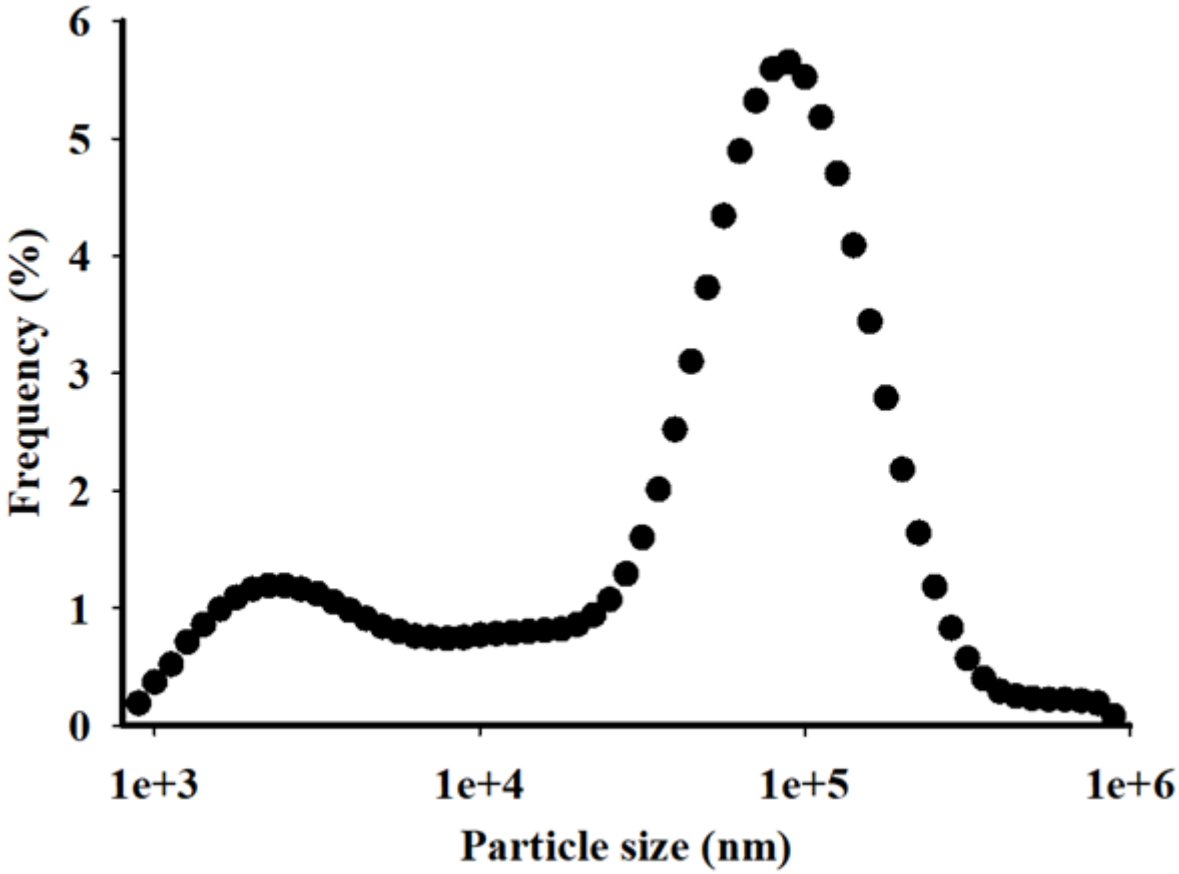

Figure 4

Particle size distribution of non-centrifuged guava juice

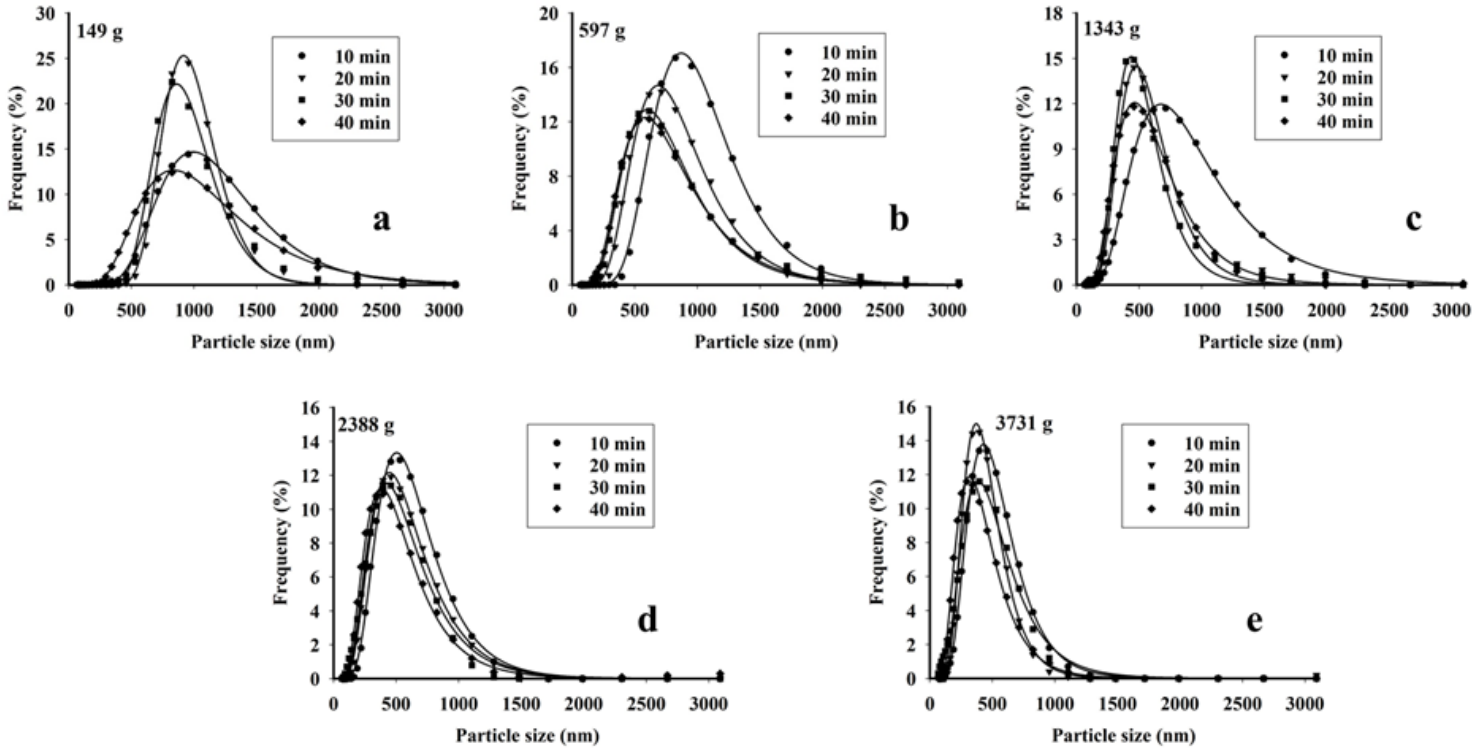

Figure 5

Particle size distribution of clarified guava juice. (a), (b), (c), (d) and (e) guava juices centrifuged at the indicated accelerations and centrifugation times.

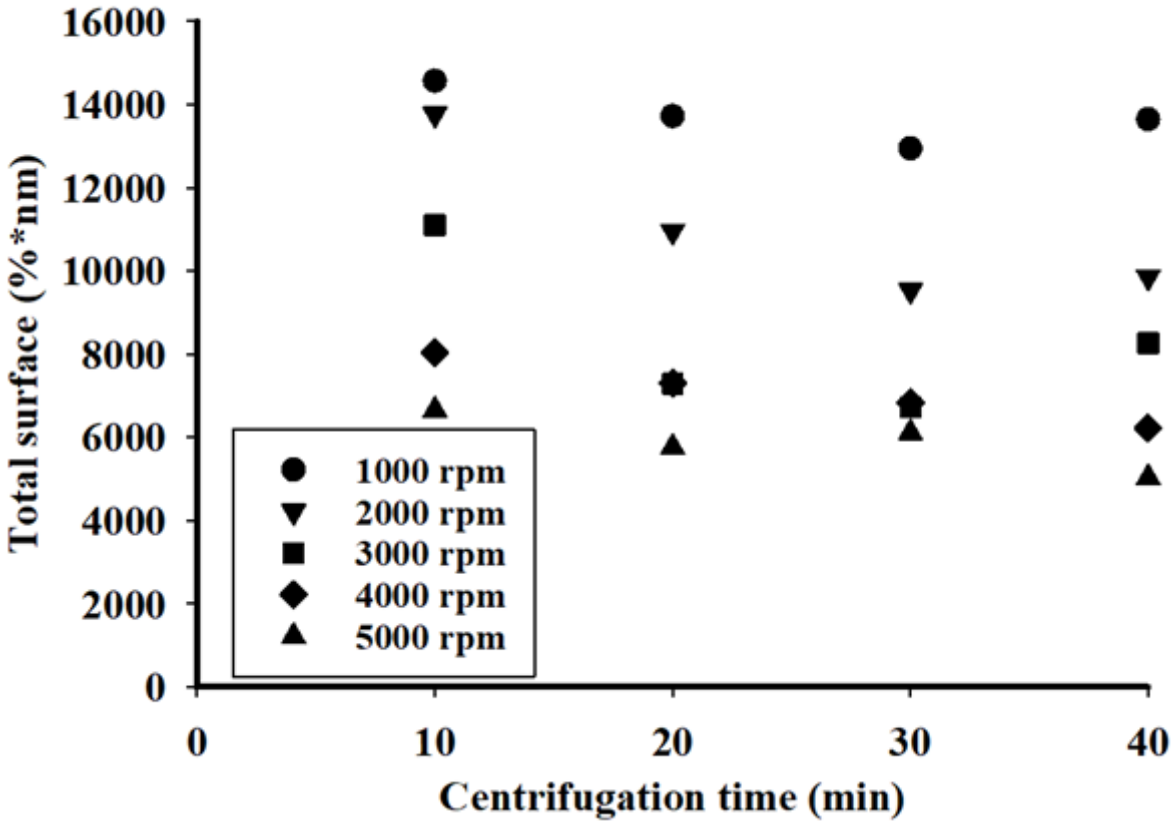

Figure 6

Particle size spectrum surface as a function of centrifugation parameters

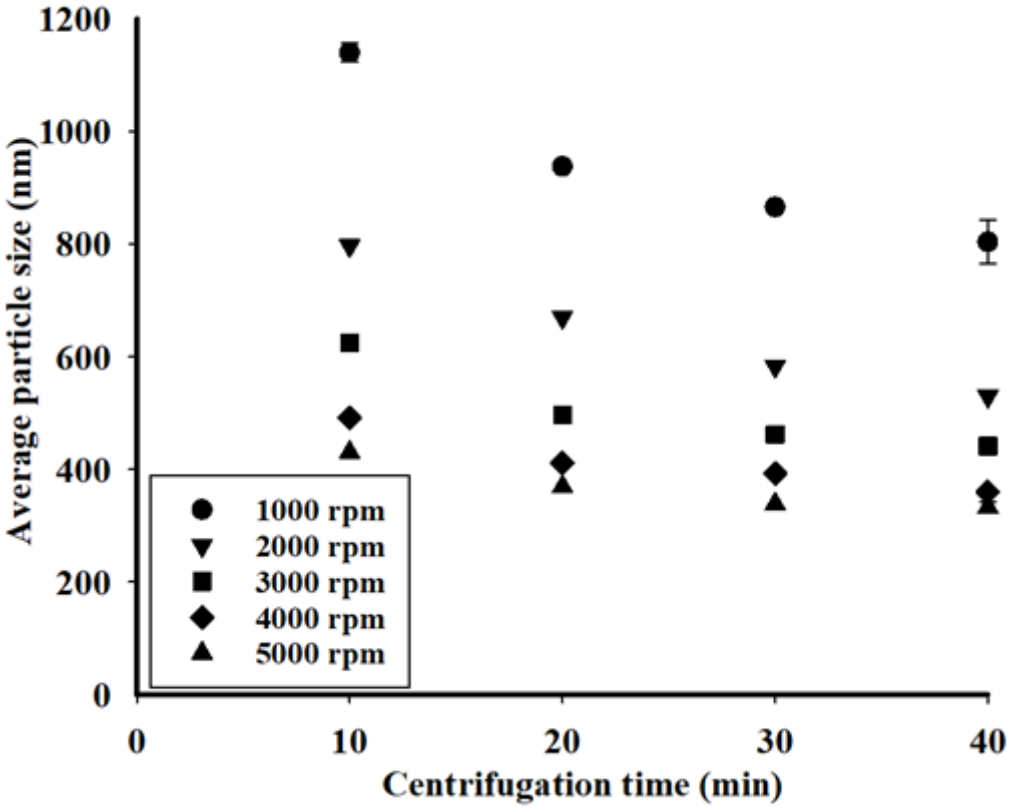

Figure 7

Average particle size of clarified juice as a function of centrifugation parameters.

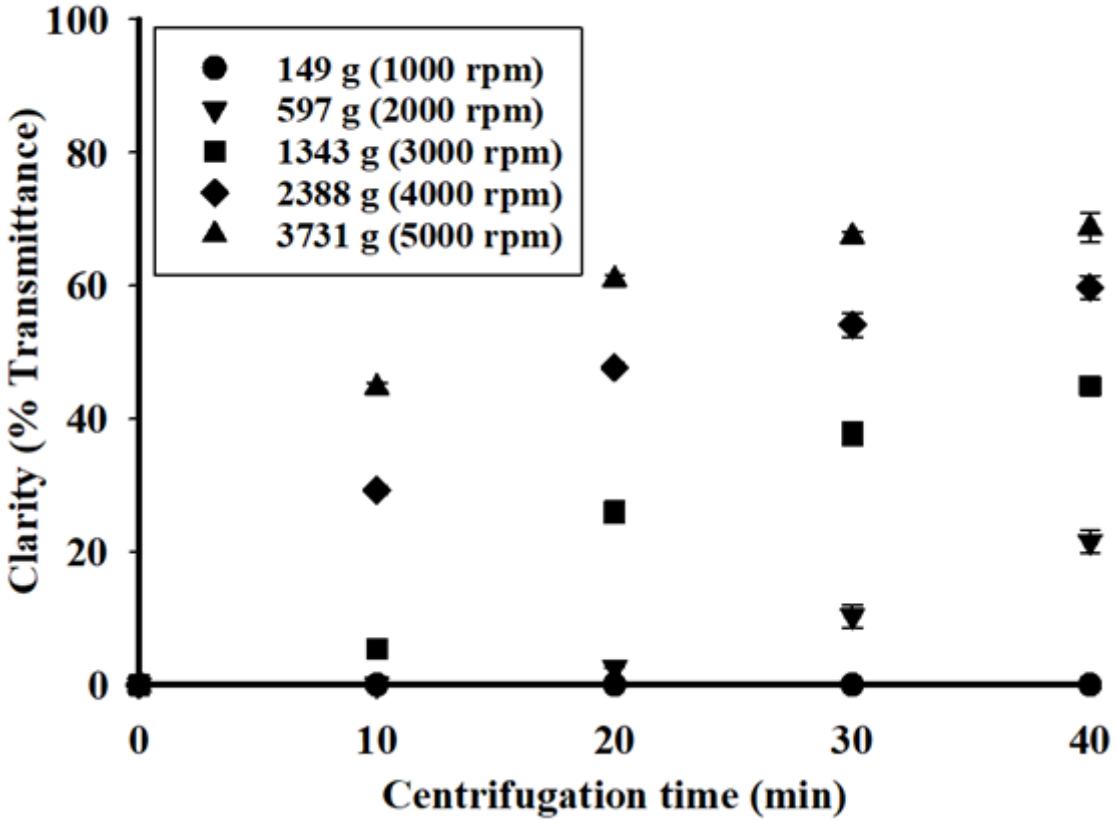

Figure 8

Clarity of guava juice as a function of centrifugation parameters

Figure 9

Pectin content of clarified guava juice as a function of centrifugation parameters

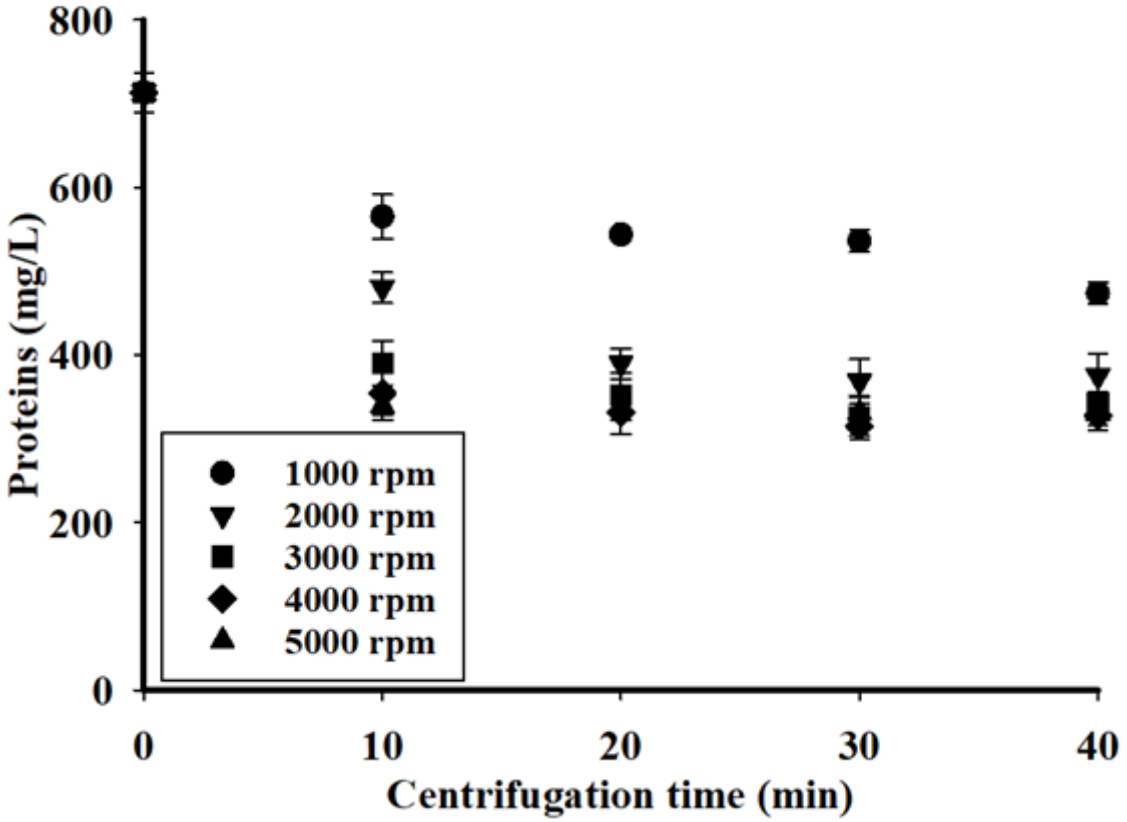

Figure 10

Protein content of clarified guava juice as a function of centrifugation parameters

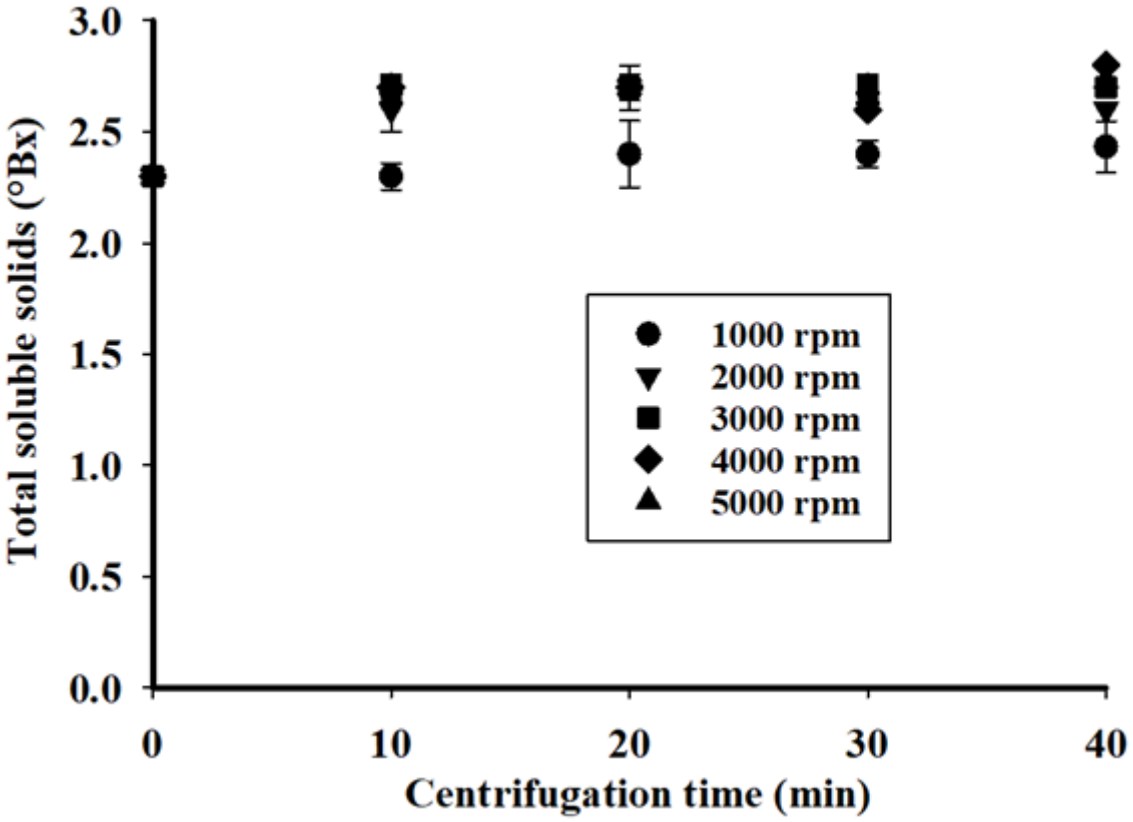

Figure 11

Total soluble sugar content of clarified juice as a function of centrifugation parameters

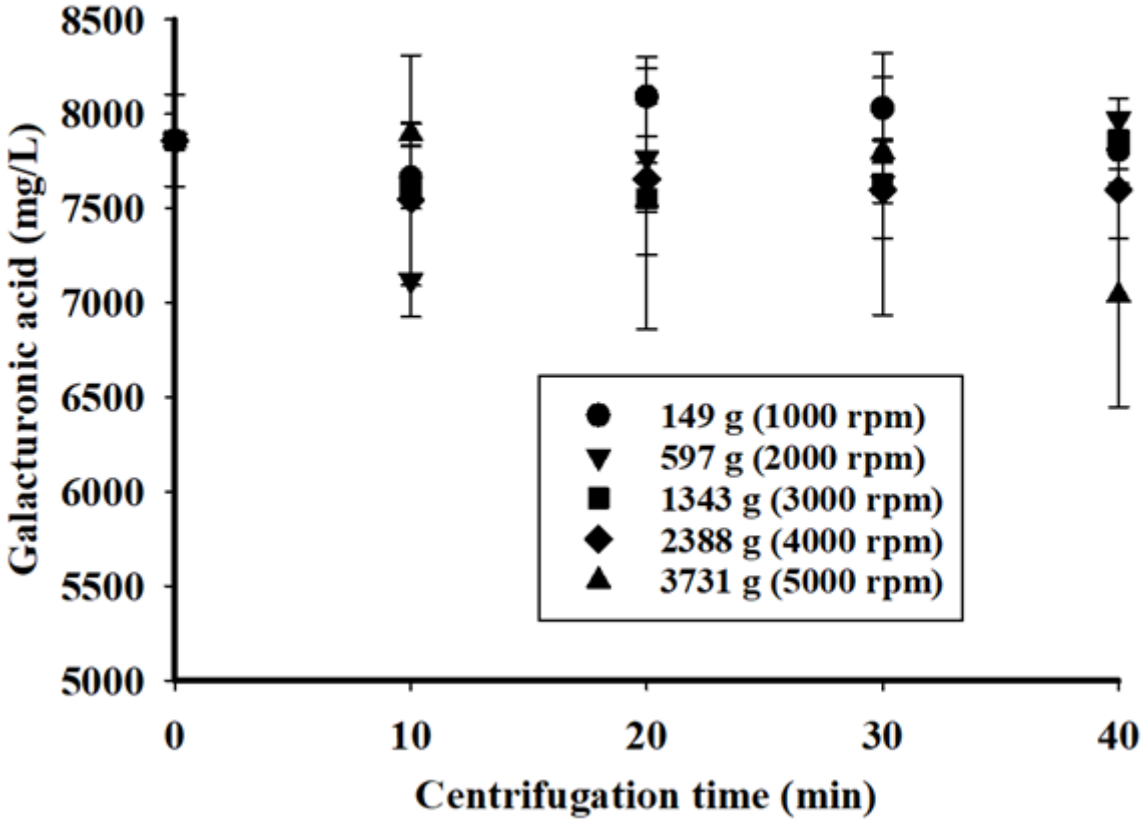

Figure 12

Galacturonic acid content of clarified juice as a function of centrifugation parameters

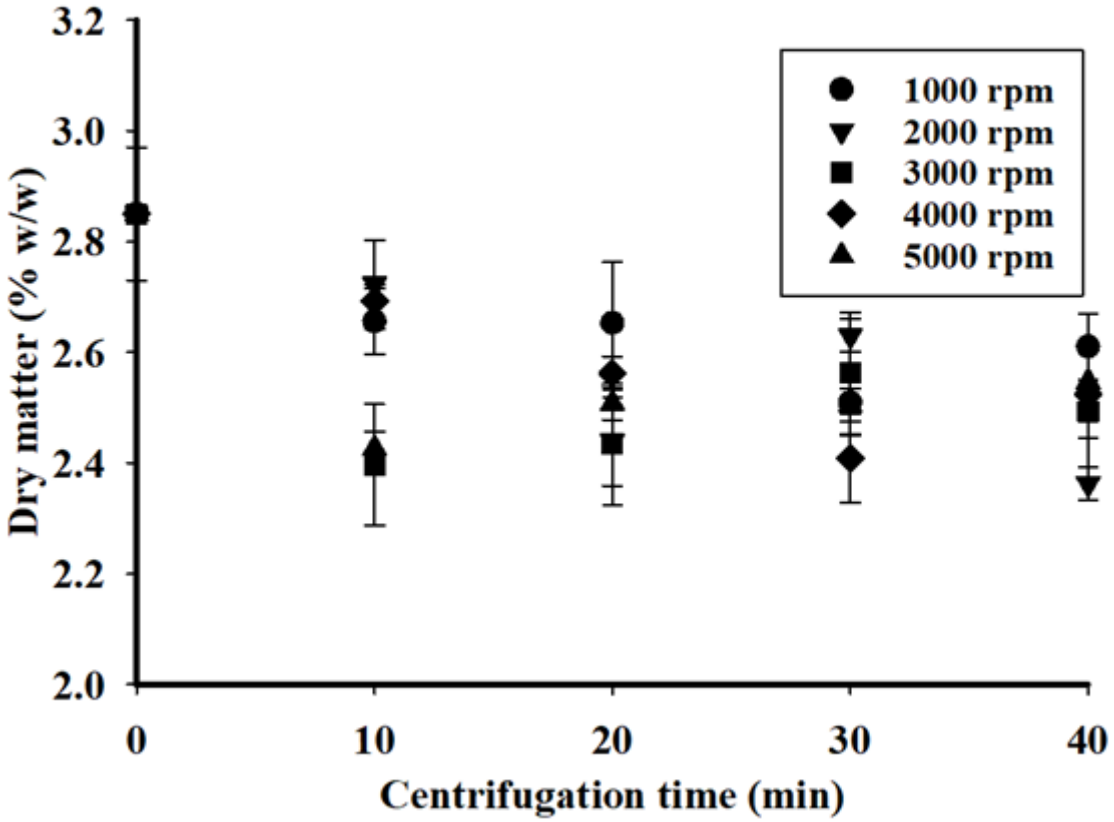

Figure 13

Dry matter content of clarified juice as a function of centrifugation parameters.

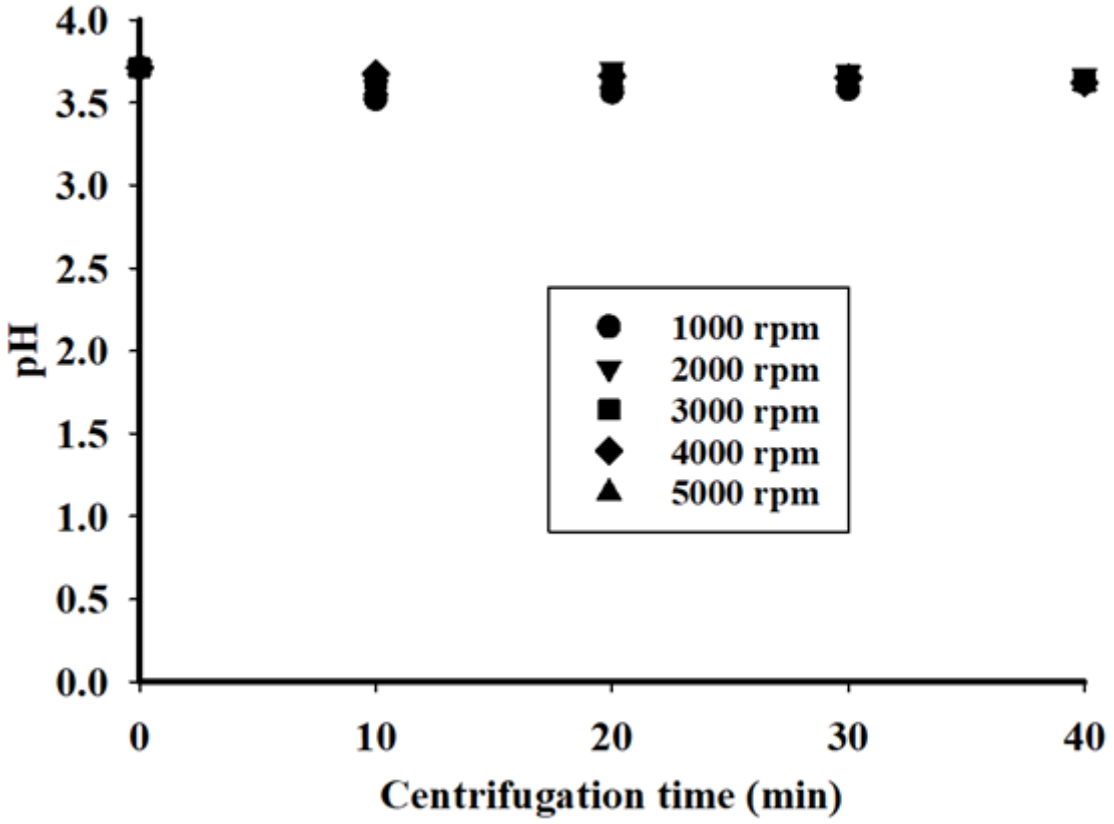

Figure 14

pH of clarified juice as a function of centrifugation parameters

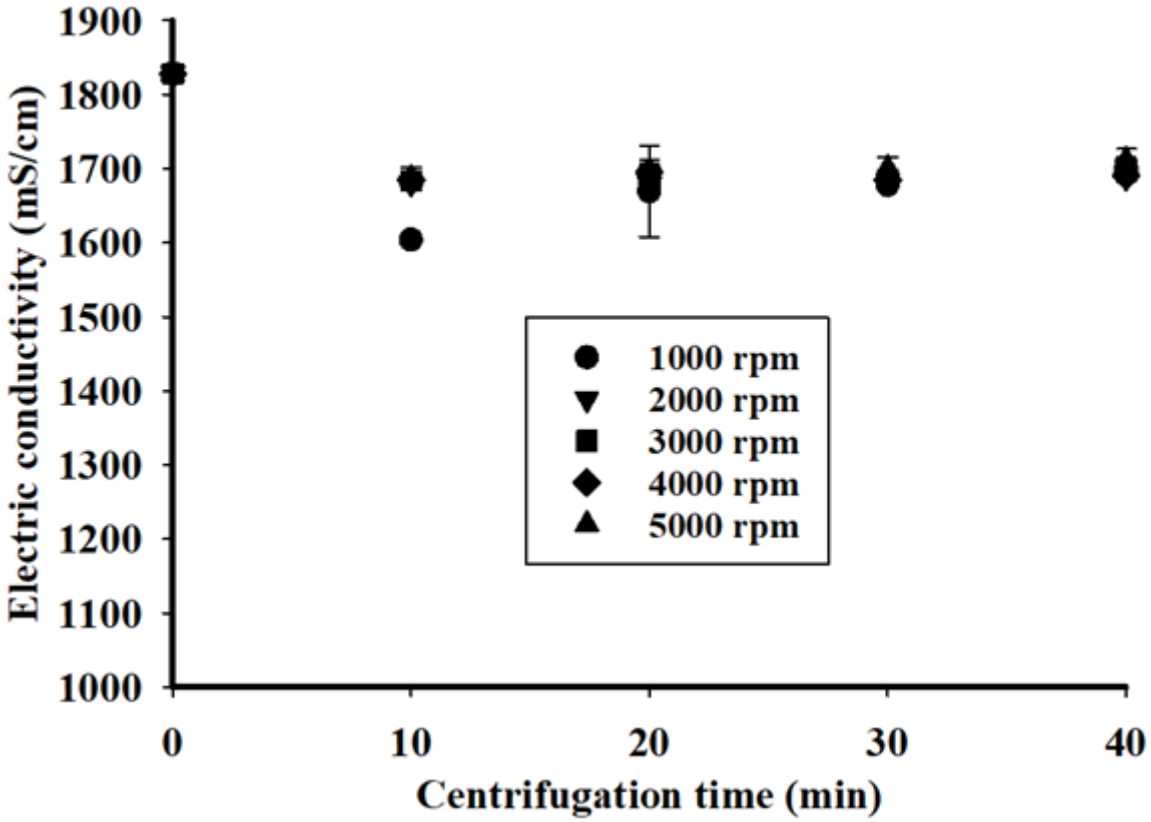

Figure 15

Electrical conductivity of clarified juice as a function of centrifugation parameters

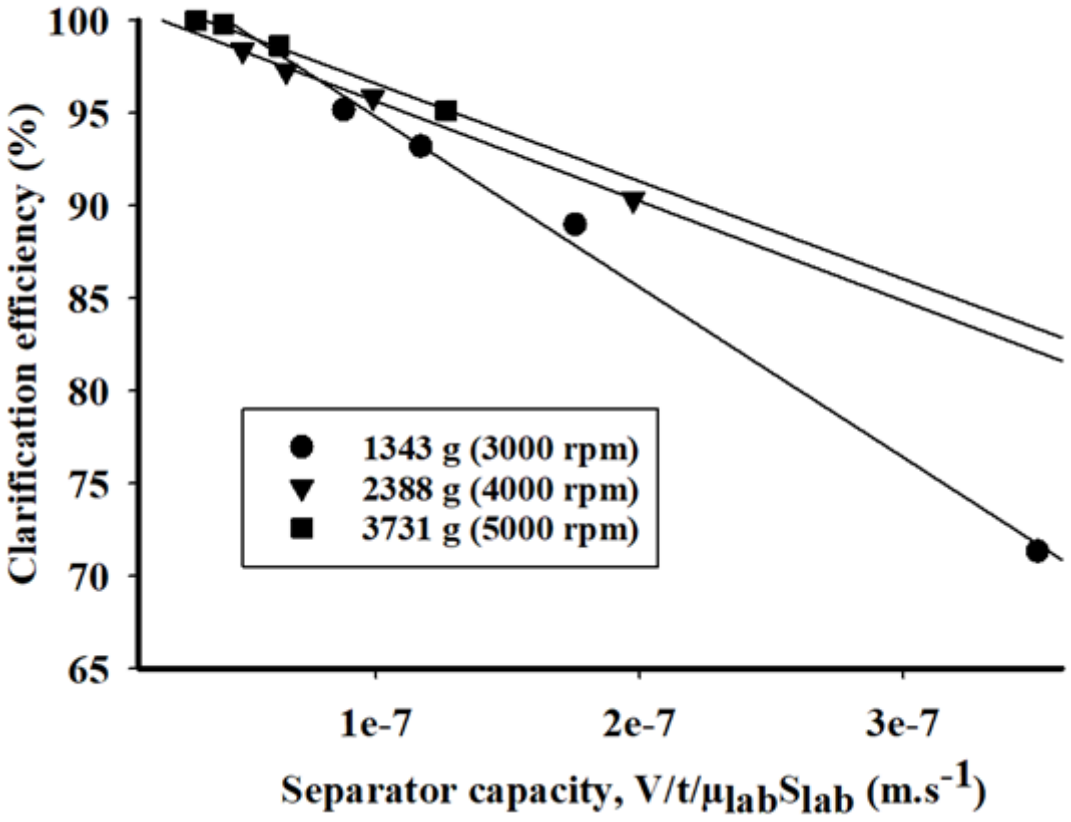

Figure 16

Performance of the laboratory centrifuge for 1343g, 2388g and 3731g.

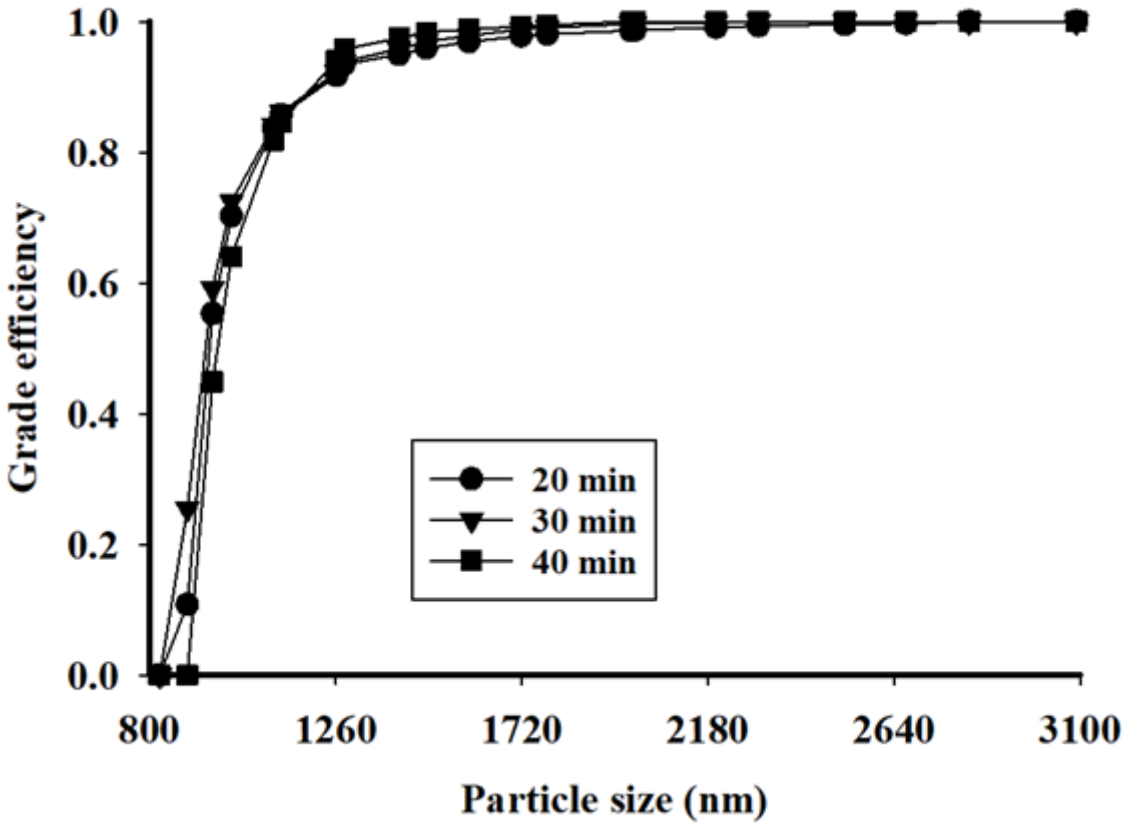

Figure 17

Variation in grade efficiency as a function of particle size for samples clarified at 1343g

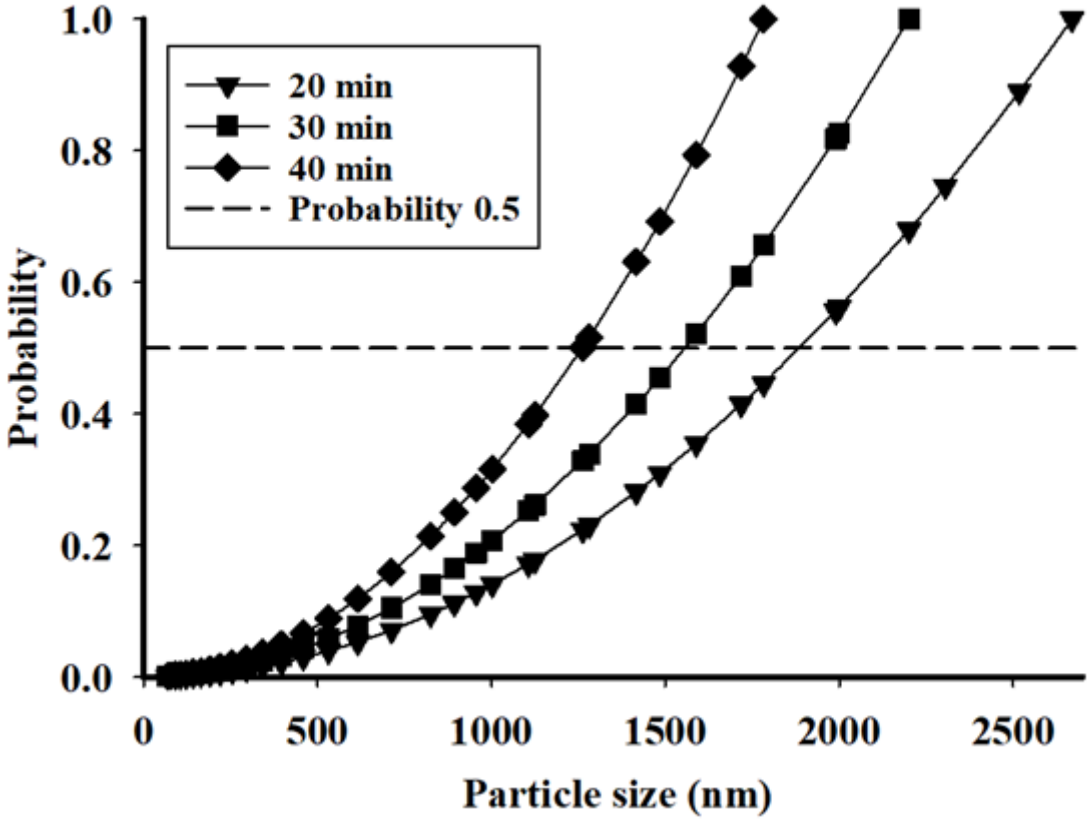

Figure 18

Probability as a function of particle size for continuous disc stack centrifuges